To be published in:
Phase Transformations and Evolution in Materials
(Proceedings: 2000 Hume-Rothery Symposium in honor of A.G. Khatchaturyan)
P.E. Turchi and A. Gonis, eds., TMS, Warrendale, Pa., 2000

ELASTIC STABILITY AND THE LIMIT OF STRENGTH

J.W. Morris, Jr.*, C.R. Krenn*, D. Roundy‡ and Marvin L. Cohen‡
*Department of Materials Science and ‡Department of Physics, University of California, Berkeley and Materials Sciences Division, Lawrence Berkeley Laboratory

Abstract

The upper limit of strength (the "ideal strength") has been an active subject of research and speculation for the better part of a century. The subject has recently become important, for two reasons. First, given recent advances in *ab initio* techniques and computing machines, the limits of strength can be calculated with considerable accuracy, making this one of the very few problems in mechanical behavior that can actually be solved. Second, given recent advances in materials engineering, the limits of strength are being approached in some systems, such as hardened or defect-free films, and their relevance is becoming recognized in others, including hard coatings, carbonitrides and diamond-cubic crystals. An elastically strained solid is always at least metastable. Given a kinetically plausible pathway, it will spontaneously transform into a sheared or broken replica of itself or into a new phase entirely. In that sense, plastic deformation is a structural phase transformation whose onset is governed by the usual criteria. It can be nucleated (and ordinarily is) but, failing that, must commence at the limit of stability of the elastic state. This thermodynamic instability sets the upper limit of strength. The present paper defines the limits of elastic stability (which are surprisingly subtle), reviews *ab initio* computations for a number of metals and compounds, shows how those limits reflect the symmetry of the strained lattice, and discusses the experimental situations in which they are known or expected to be important.

Introduction

While one does not ordinarily list "mechanical strength" among the subfields of the theory of phase transformations, there are perfectly valid reasons to do so. As Gibbs [1] noted more than a century ago, a solid that is subject to a deviatoric (shear) stress is always at least metastable with respect to transformation into a "stress-free" state (free, that is, of the deviatoric stress that drives plastic deformation). If the solid is crystalline, the transformation to a stress-free state is accomplished by one of three basic mechanisms (Fig. 1): (1) The solid deforms into a sheared replica of itself by moving dislocations, twinning, or diffusion. (2) The solid breaks into stress-free fragments. (3) The solid changes its shape by changing its crystal structure, a process that is sometimes called "transformation-induced plasticity". The strength of the solid is the stress that triggers the easiest of these transformations.

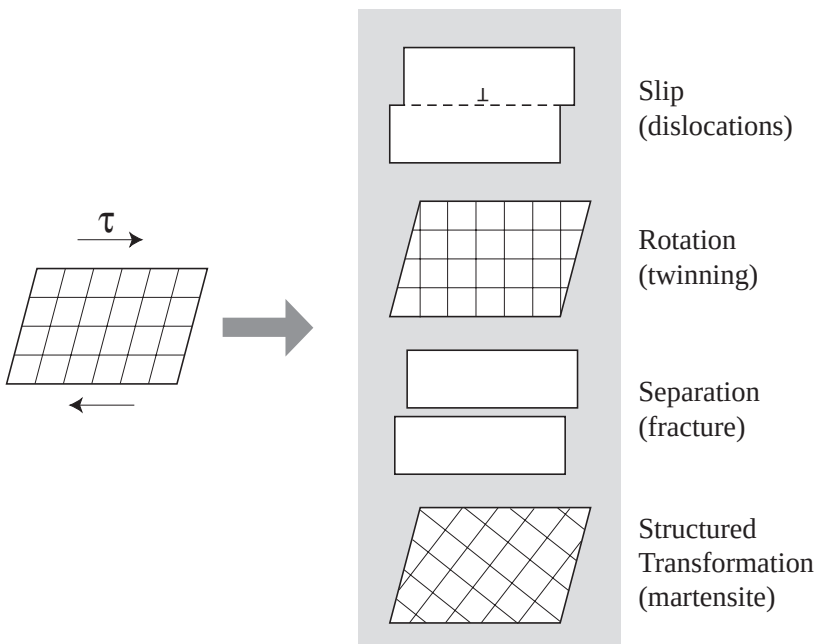

Fig. 1: Deformation mechanisms (diffusional creep should be added to complete the list).

There are three ways to start a structural transformation: heterogeneous nucleation, homogeneous nucleation and thermodynamic instability. Mechanical deformation usually nucleates heterogeneously at pre-existing dislocations, cracks or internal stress concentrations. If no such defects exist, or if they are very difficult to activate, a solid deforms when the applied stress is large enough to nucleate defects spontaneously or to destabilize the lattice itself. The stress that is just sufficient to destabilize the lattice (the elastic limit) is the upper limit of strength; no solid can survive unchanged if the stress can disrupt the atomic bonds that hold it together.

Early research on the elastic limit, or "ideal strength" is summarized by Kelly and Macmillan [2]. Separate lines of inquiry considered fracture in tension and failure in shear. The ideal strength of a crystal loaded in tension was studied by a series of investigators from Polanyi [3] and Zwicky [4] through Born and Furth [5] to Orowan [6] and others [2]. Most of these investigators [3,4,6-11] used Born-Mayer or Lennard-Jones central-force potentials to investigate the elastic instabilities that lead to fracture in tension.

The simple, textbook estimate of the ideal tensile strength was done by Orowon [6]. He assumed that the stress required to separate planes of atoms is a sinusoidal function of their displacement, and is proportional to Young's modulus when the displacement is small. Since the net work required for brittle cleavage is at least twice the surface tension (γ), the cleavage stress, σ_m, is approximately

$$\sigma_m = \sqrt{\frac{E\gamma}{h}} \approx 0.3E \tag{1}$$

where E is the modulus and h is the interplanar separation in the direction of tension. The factor 0.3 follows from a rough estimate of the surface tension. The strength predicted by eq. (1) is significantly higher than that estimated by other methods, but is still a useful reference value.

Research into the ideal shear strength can be traced back to Frenkel [12], whose model remains the textbook case [2]. He considered the rigid shear displacement of neighboring planes of atoms, and assumed that the shear stress-shear strain relation is sinusoidal, with period, b, which is the interatomic distance in the direction of shear. In the limit of small displacement, x, the shear stress, τ, is linear in the strain; $\tau = Gx/h$, where G is the shear modulus in the plane of shear and h is the interplanar separation. This limit, together with the sinusoidal approximation for τ, fixes the function $\tau(x/b)$. Its maximum value is the ideal strength in shear:

$$\tau_m = \frac{Gb}{2\pi h} \tag{2}$$

The most familiar case is $\langle 11\bar{2}\rangle\{111\}$ slip in fcc crystals, for which $\tau_m \approx G/9$.

Frenkel's model was revisited by Mackenzie [13], who predicted significantly smaller values of τ_m. However, until fairly recently there were very few atomic-level calculations of the ideal strength in shear. Macmillan and Kelly's work on NaCl and Ar [7-8], and Huang, Milstein and Baldwin's study of shear in Ni [14] are among the few examples.

The experimentalists who were interested in the ideal strength studied the behavior of defect-free whiskers [2]. While interesting results were obtained from this research, particularly from Brenner's [15] classic work on Fe, Cu and Ag, the samples are difficult to prepare and test, and the physical meaning of the results is not entirely clear. Recent

theoretical calculations and nanoindentation experiments suggest that the maximum strengths measured in whiskers are well below the ideal strength.

In the last few years there has been a significant increase of interest in the ideal strength, by theorists, experimentalists and practicing metallurgists. Theorists have returned to the problem because it appears that it can now be solved. Advances in theoretical techniques and computing machines make it possible to calculate the limits of elastic stability with some confidence. Experimentalists have returned to the problem because strengths that seem to approach the ideal are now being measured in nanoindentation experiments that test the actual hardness of local regions in thin films. Practical metallurgists are interested in the problem because ultra-small volumes and ultrahard materials are increasingly important in engineering devices, and the ideal strength is relevant to both. Finally, materials scientists are learning that the conditions of elastic stability provide a simple framework for understanding a number of puzzling phenomena in mechanical behavior. Examples include the tendency of bcc materials to cleave on {100} and slip along ⟨111⟩ in a variety of planes, the tendency of fcc materials to remain ductile at low temperature while bcc's do not, and the tendency of diamond cubic materials to transform rather than yielding under indentation loads.

In the following we give a brief summary of recent progress in the field, focusing on work done since the appearance of Kelly and Macmillan's 1986 monograph [2], and on the results and implications of the *ab initio* calculations that have recently become possible. We discuss this work under four headings: (1) The conditions of elastic stability. Perhaps surprisingly, the basic concepts of elastic stability and ideal strength are subtle, and the definition of the ideal strength is not settled. (2) Computing the ideal strength. Calculations have been done for a sufficient number of solids to identify several interesting trends. (3) Understanding the ideal strength. The ideal strength is set by the limits of elastic stability. In the usual case these limits are not arbitrary, but are fixed by the symmetry of the underlying crystal and the change in symmetry with deformation. The overriding influence of symmetry not only explains when instabilities occur, but also explains why the strengths of materials with a given crystal structure can be written in a simple dimensionless form. (4) Achieving the ideal strength. It is becoming increasingly clear that there are materials and load geometries in which the ideal strength governs mechanical behavior. There are others in which the ideal strength is inherently unattainable.

Conditions of elastic stability

A material is tested for its strength by placing it in some testing device and straining it until it deforms plastically or breaks. If we assume constant temperature and control the strain, the governing thermodynamic potential is the Helmholtz free energy, F. However, the solid is acted on by the loading mechanism, which does work during any displacement of its boundary. Thermodynamic equilibrium requires that in any change of state at constant temperature the increase in free energy equal or exceed the work done by the loading mechanism [16]:

$$\delta F \geq \delta W \tag{3}$$

The first-order form of eq. (3) sets the conditions of mechanical equilibrium, which require that the tractions on the solid surfaces be equal and opposite. Mechanical stability is governed by the second-order terms. But the second-order terms depend on how the tractions vary with the strain, and this is a function of the loading mechanism. Hence, as Hill [16] and Hill and Milstein [17] have discussed in some detail, elastic stability depends on the behavior of the loading mechanism as well as on the properties of the material.

Hill [16] suggests that one define an *intrinsic* strength by selecting a convenient measure of the stress (such as the Cauchy stress or the Green stress that is conjugate to the Lagrangian strain) and assuming a loading mechanism that maintains that stress to at least second order. The problem is that the result depends on which stress is chosen. Perhaps the most appealing choice is the Cauchy ("true") stress (Wang, et al. [18-20]), but there are other candidates [16]. In practice, different choices of reference stress produce very similar numbers for the ideal strength in tension or shear (basically because, with the exception of tests done under high pressure, the stress at instability is small compared to the elastic modulus). Still, it is troublesome that one must choose a reference stress, particularly since it may not be easy to design a practical loading mechanisms that maintains it.

Internal stability and ideal strength

A useful, unique definition of the intrinsic strength is implicit in Gibbs' [1] original formulation of the conditions of stability. Gibbs sought the conditions that must be satisfied for stability with respect to internal changes. These *conditions of internal stability* are always necessary; a system that is rendered unstable by internal perturbations must evolve whatever the mechanism loading its boundary. In our case Gibbs' condition of internal stability is

$$\delta F \geq 0 \tag{4}$$

where the variation is to be taken at constant temperature with boundaries fixed in space.

The consequences of eq. (4) are developed in ref. [21]. We confine ourselves here to stating the result. Let the free energy of a solid of fixed composition be written as a function of the temperature and the Lagrangian (Green's) strain: $F = \tilde{F}(T, \mathbf{E})$. The Lagrangian stress and the elastic moduli are defined by the first and second derivatives:

$$\tau_{ij} = \frac{1}{V_0}\left[\frac{\partial \tilde{F}}{\partial E_{ij}}\right] \tag{5}$$

$$C_{ijkl} = \frac{1}{V_0}\left[\frac{\partial^2 \tilde{F}}{\partial E_{ij}\partial E_{kl}}\right] \tag{6}$$

where V_0 is the volume of the reference (unstrained) state. Now suppose that the solid is given an infinitesimal strain, $\varepsilon_{ij} = 1/2(\delta u_{i,j}+\delta u_{j,i})$, from a reference state in which the stress is τ_{ij}. The Cauchy ("true") stress, t_{ij}, is related to the infinitesimal strain, $\boldsymbol{\varepsilon}$, by

$$t_{ij} = \tau_{ij} + B_{ijkl}\varepsilon_{kl} \tag{7}$$

where **B** is the Wallace tensor [22],

$$B_{ijkl} = C_{ijkl} + \frac{1}{2}[\tau_{jk}\delta_{il} + \tau_{ik}\delta_{jl} + \tau_{jl}\delta_{ik} + \tau_{il}\delta_{jk} - 2\tau_{ij}\delta_{kl}] \tag{8}$$

The terms involving the stresses on the right-hand side of eq. (8) are second-order terms introduced by the translation from the Lagrangian strain to the infinitesimal strain, ε_{ij} [19,21-22].

Internal stability requires that the symmetric part of **B**, the tensor $\boldsymbol{\lambda}$, have no negative eigenvalues. Since [21]

$$\lambda_{klmn} = C_{klmn} + \frac{1}{2}\ [\tau_{km}\delta_{ln}+\tau_{kn}\delta_{lm}+\tau_{lm}\delta_{kn}+\tau_{ln}\delta_{km}-\tau_{kl}\delta_{mn}-\tau_{mn}\delta_{kl}] \tag{9}$$

$\boldsymbol{\lambda}$ has Voigt symmetry and can, therefore, be written as the symmetric, 6x6 matrix, λ_{ij}. Let λ_α ($\alpha = 1,...,6$) be the eigenvalues of λ_{ij}. For all α,

$$\lambda_\alpha \geq 0 \tag{10}$$

If a material is loaded from a relaxed initial state the strength in the direction of the load cannot exceed the value set by the first violation of the condition (10). This is, hence, a good, intrinsic measure of the ideal strength. (Wang, et al. [19] have shown that the same result is obtained if one assumes a loading mechanism that maintains the Cauchy stress and applies condition (3)).

As a specific example, consider a cubic crystal stretched in uniaxial tension along [100]. The crystal becomes tetragonal as soon as it is stretched, and the elastic matrices c_{ij} and λ_{ij} reflect this. The conditions of stability are [21]:

$$(c_{11}+\sigma)(c_{22}+c_{33}) \geq 2(c_{12}-\sigma/2)^2 \tag{11}$$

$$c_{22} \geq c_{23} \tag{12}$$

$$c_{44} \geq 0 \tag{13}$$

$$c_{55} \geq -\ \sigma/2 \tag{14}$$

where the c_{ij} are the elastic moduli in the Voigt notation, and σ is the applied stress. The conditions that govern other stress states are easily found. They only have simple algebraic expressions when the principle stresses are along axes of high symmetry.

It is important to note that the conditions (10) test the internal stability of the current state, which is characterized by the Cauchy stress, **t**, and by the current values of the elastic constants, c_{ij}. Eqs. (10) are not capable of finding instabilities *a priori* since they do not reveal instabilities that are displaced from the current state by a finite strain. For example, the conditions contained in eqs. (11-14) govern the stability of a strained solid whose current state (and, hence, matrix of elastic constants) has tetragonal symmetry. These conditions do not identify the instability in shear on {111} that is the normal mode of plastic failure in an fcc crystal pulled in [100] tension. Instability in shear on {111} requires a finite shear in a {111} plane, which is a triclinic or monoclinic distortion governed by elastic constants that have that symmetry. Elastic instability and, hence, the ideal strength depends on the deformation mode.

Extrinsic stability and "engineering" strength

When the loading mechanism controls some stress other than the Cauchy stress it may impose conditions of stability that are more stringent than those contained in eq. (10), with the consequence that the largest possible value of the effective "engineering" strength is significantly less than the ideal. An important example is stability under "all around dead loading" (Hill [16]). In dead loading the loading mechanism fixes the "engineering stress" (the Piola-Kirkhoff stress in the language of continuum mechanics), which is the applied force per unit area of the reference configuration. Since the Piola-Kirkhoff stress tensor need not be symmetric a material under dead loading must be stable with respect to rotation as well as strain.

The full set of stability conditions under dead loading is presented and discussed by Hill [16]. The conditions that govern stability with respect to rotation are stringent. Among them, if σ_i (i=1,2,3) are the Cauchy principle stresses set by a "dead" loading mechanism, we must have

$$\sigma_i + \sigma_j > 0 \qquad (i \neq j = 1,2,3) \tag{15}$$

That is, the stress system must produce a net tension.

"Soft phonons"

From the perspective of the crystal lattice, mesoscopic to macroscopic elastic deformations fall at the long-wavelength end of the vibrational spectrum. Behavior at shorter wavelengths is also important, for at least two reasons. First, vibrational instabilities ("soft phonons") may intrude before long-range elastic instability, as happens in some martensitic phase transformations [23]. Second, even when the instability is long-range, its initial development may still be dominated by a "critical wave" with a much shorter wavelength, as happens in other thermodynamic instabilities (e.g., spinodal decomposition). The

crystallographic type and wavelength of this critical wave may determine how the instability ultimately resolves itself, whether as a shower of dislocations or twins, cleavage, or structural transformation.

While many investigators have studied "soft mode" instabilities in unstressed solids undergoing thermal phase transitions, the authors have found very little work on the vibrational behavior of highly strained solids. Pertinent investigations include that of Wallace [22], who studied the criteria that govern vibrational stability in strained solids, and those of Wang, et al. [20], who used molecular dynamic simulations of model systems to investigate behavior just after the onset of instability.

Computing the ideal strength

Methodology

With modern computers and theoretical techniques it is possible to do accurate *ab initio* calculations of the energies of aggregates of several hundred atoms. Since the elastic behavior of a perfect crystal can be computed from the behavior of a single unit cell the available techniques are adequate to calculate the elastic properties of the elements and typical ordered compounds, at least in the low-temperature limit [24].

The ability to compute the energy and the elastic constants makes it possible, in theory, to use the conditions set by eq. (10) to find the ideal strength along any equilibrium load path. To do this, it is neither practical nor necessary to compute the full matrix of elastic constants at each incremental step. All attempts at first-principles calculation known to us take the simpler approach of incrementing a single strain until the stress reaches its maximum value. The uniaxial deformation is carried out in one of two ways: uniaxial strain or uniaxial stress. Choosing ε_α as the infinitesimal strain increment, the change in the conjugate Cauchy stress (t_α) is given by

$$dt_\alpha = \lambda_{\alpha\alpha} d\varepsilon_\alpha \qquad \text{(uniaxial strain)} \qquad (16)$$

$$dt_\alpha = \beta_{\alpha\alpha} d\varepsilon_\alpha = \frac{1}{s_{\alpha\alpha}}\, d\varepsilon_\alpha = \frac{|\boldsymbol{\lambda}|}{\lambda^{\alpha\alpha}}\, d\varepsilon_\alpha \qquad \text{(uniaxial stress)} \qquad (17)$$

where $|\boldsymbol{\lambda}|$ is the determinant of $\boldsymbol{\lambda}$ and $\lambda^{\alpha\alpha}$ is the cofactor of the element $\lambda_{\alpha\alpha}$.

In the former case, uniaxial strain, the maximum stress does not fall at an intrinsic instability, and is not a very good approximation to the intrinsic strength unless the material is almost isotropic.

In the latter case, uniaxial stress, the maximum of the Cauchy stress is an intrinsic instability. However, it is not necessarily the first instability to be encountered along the deformation path. If $\boldsymbol{\lambda}$ and $\lambda^{\alpha\alpha}$ have common eigenvalues, the zeros of these eigenvalues divide out of eq. (17) and do not produce maxima in the applied stress, t_α. Physically, if $\boldsymbol{\lambda}$

has eigenvectors whose deformations are orthogonal to ε_α (i.e., do not change ε_α), their instabilities terminate stable deformation along ε_α without producing an extremum in the stress conjugate to ε_α. Orthogonal instabilities are particularly likely when ε_α is along an axis of high symmetry. For example, when fcc crystals are stretched along [100] the orthorhombic instability ($c_{22} = c_{23}$) is usually reached before the tensile instability. Orthogonal instabilities are less common in shear strains that significantly reduce the crystal symmetry, and are relatively easy to detect when they occur.

In practice one can test for orthogonal instabilities in either of two ways. First, the full set of eigenvalues can be probed periodically along the deformation path. Since the eigenvalues are, ordinarily, well-behaved functions of the strain, it is usually straightforward to determine when and where zeros occur. Second, the atomic configuration can be perturbed to introduce orthogonal strains and test stability directly. This method is easily incorporated into tests in uniaxial stress that use atom displacements to relax the lateral stresses after each strain increment.

Results

The "first-principles" calculations of the ideal strength that known to us can be gathered into two sets: strength in shear and strength in tension.

Strength in shear. The first *ab initio* investigation of ideal strength in shear that is known to us was that by Paxton, et al. [25] almost a decade ago. They used approximate pseudopotential methods to calculate the ideal shear strength in uniaxial strain. The materials studied included the bcc metals V, Nb, Cr, Mo and W sheared in the system ⟨111⟩{112}, and the fcc metals Al and Cu sheared in the system ⟨112⟩{111}. Some of the results are included in Table I. In general, they found bcc shear strengths in the range 0.14-0.17G_u, and fcc strengths 0.14G_u for Al and 0.13G_u for Cu, where $G_u = (1/3)[c_{11}-c_{12}+c_{44}]$ is the shear modulus for unrelaxed strain, and has the same value for the systems ⟨111⟩{112} and ⟨112⟩{111}.

Xu and Moriarty [26] calculated the unrelaxed shear strength (uniaxial strain) for Mo, and for Na and Mg in the bcc structure. They used four-body potentials extracted from generalized pseudopotential theory by a method of their own construction. They found a value of 0.17G_u for the shear strength of Mo, which is about 20% above Paxton, et al. [25]. They found much lower shear strengths for bcc Mg (0.1G_u) and Na (0.08G_u). Söderlind and Moriarty [27] computed the unrelaxed shear strength of Ta in the system $[111](11\bar{2})$ as a function of pressure to 10 Mbar. Their value for atmospheric pressure, 7.37 GPa (0.105G_u) is included in Table I. This value is, in dimensionless form, well below that calculated for the other transition metals. Interestingly, they calculate a significant increase in strength with pressure, which is primarily due to an increase in the dimensionless strength. Their predicted value of the unrelaxed strength at 0.45 Mbar is 0.123G_u.

Table I: *Ab initio* calculations of the ideal strength in shear.
τ_u refers to the unrelaxed case, τ_r to the fully relaxed case.

Material	Cell	Ref	System	τ_u (GPa)	τ_u/G_u	τ_r (GPa)	τ_r/G_r
Al	fcc	25	$[11\bar{2}](111)$	3.50	0.14		
		28	$[11\bar{2}](111)$	3.40	0.13	1.85	0.084
Cu	fcc	25	$[11\bar{2}](111)$	5.3	0.13		
		28	$[11\bar{2}](111)$	4.00	0.10	2.65	0.088
Ir	fcc	25	$[11\bar{2}](111)$	24.12	0.12		
W	bcc	25	$[111](11\bar{2})$	19.2	0.12		
		30	$[111](11\bar{2})$	19.2	0.12	18.1	0.11
		30	$[111](1\bar{1}0)$	20.8	0.13	17.7	0.11
		30	$[111](12\bar{3})$	19.6	0.12	17.7	0.11
Mo	bcc	25	$[111](11\bar{2})$	17.8	0.13		
		26	$[111](11\bar{2})$	20.9	0.17		
		31	$[111](11\bar{2})$	16.4	0.12	15.6	0.12
Cr	bcc	25	$[111](11\bar{2})$	20.5	0.16		
Nb	bcc	25	$[111](11\bar{2})$	7.52	0.16		
V	bcc	25	$[111](11\bar{2})$	7.28	0.14		
Ta	bcc	27	$[111](11\bar{2})$	7.37	0.105		
Na	bcc	26	$[111](11\bar{2})$	0.20	0.08		

Our own calculations have included shear strengths of the fcc metals Al and Cu [28-29] and bcc metals W [30] and Mo [31] in both unrelaxed and relaxed shear (uniaxial stress). The results are included in Table I. The strengths in the relaxed case are found by imposing an incremental shear strain in the designated slip system ($\langle 11\bar{2}\rangle(111)$ in the fcc case), adjusting the five orthogonal strains until all stresses except the shear stress conjugate to the primary strain vanish (as calculated by the Hellman-Feynman method), and iterating this procedure until the shear stress reaches its maximum value.

For the fcc metals, the unrelaxed strengths are 3.4 GPa ($0.13G_u$) for Al and 4.0 GPa ($0.10G_u$) for Cu, somewhat below the values computed by Paxton, et al. [25]. The relaxed strengths are much lower still, 1.85 GPa ($0.084G_r$) for Al and 2.65 GPa ($0.088G_r$) for Cu, where the modulus $G_r = 3c_{44}(c_{11}-c_{12})/4c_{44}+c_{11}+c_{12}$. The shear stress-strain curves are plotted in Fig. 2, and show the dramatic effect of the relaxation. The strains at shear instability in the relaxed case are shown in Table II. Despite the similarity of the dimensionless shear strengths of Al and Cu, the relaxation strains are very different. The cause seems to lie in the very different elastic anisotropies of the two metals [29].

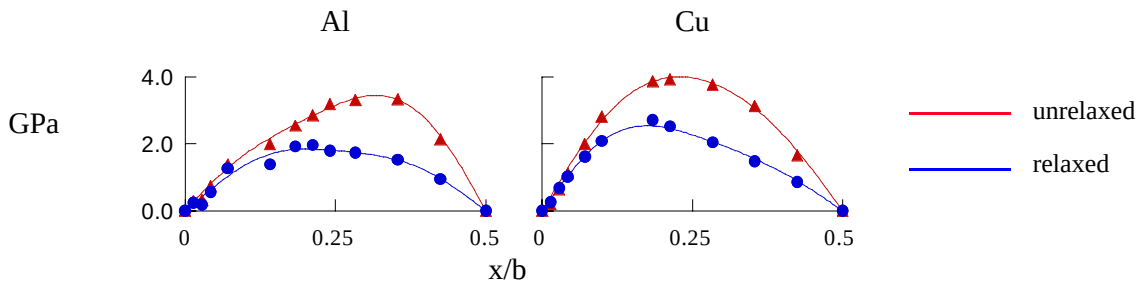

Fig. 2: Shear stress-strain curves for Al and Cu sheared on $[11\bar{2}](111)$. x/b is the atomic displacement along $[11\bar{2}]$.

Table II: Engineering shear strains at failure for Al and Cu in a coordinate system spanned by axes along [111], $[1\bar{1}0]$ and $[11\bar{2}]$ [27,28].

	γ^E_{13}	ε^E_{11}	ε^E_{22}	ε^E_{33}	$\Delta V/V_0$
Al	14.5	1	-3	3	1.4
Cu	13	-3	3	0.2	0.4

For the bcc metals, the most striking observation is the similarity of the relaxed shear strengths of W for the three common bcc slip systems: τ_r = 18.0 GPa for ⟨111⟩{110} and 17.7 GPa for ⟨111⟩{112} and ⟨111⟩{123} (Fig. 3). In all three cases the shear strain at instability is about 0.17. We shall discuss the physical reason for this similar behavior in the next section. Comparing slip in W and Mo on the system ⟨111⟩{112}), the relaxed strengths are 17.7 GPa ($0.11G_r$) and 15.6 GPa ($0.12G_r$) respectively, where $G_r = 3c_{44}(c_{11}-c_{12})/(4c_{11}+(c_{11}-c_{12}))$. The unrelaxed values are 18.7 and 16.4 GPa, respectively, close to those found by Paxton, et al. [25]. In dimensionless form, both strengths are $0.12G_u$, where $G_u = (1/3)(c_{11}-c_{12}+ c_{44})$.

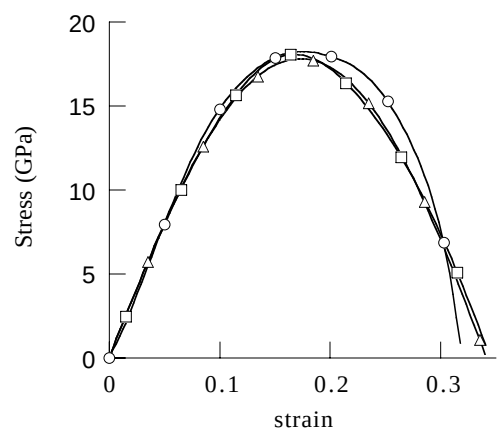

Fig. 3: Shear stress-strain curves for W: circles = {110}, squares = {112}, triangles = {123}.

Strength in tension. We begin the discussion of recent calculations of strength in tension with the work of Milstein and Chantasiriwan [32], who used fitted embedded-atom (EAM) methods to compute the response of twelve fcc and bcc metals to unconstrained uniaxial loading along [100], [110] and [111]. Their subjects included the fcc metals Al, Cu, Ni, Au, and Ag, and the bcc metals Mo, Na, Li, Rb, Nb and Fe. While their potential is imprecise by the standards of recent pseudopotential work, its simplicity allowed them to explore the behavior of a number of metals in a number of different deformation modes. A sampling of their results is included in Table III. They found that bcc metals are weak in tension when pulled along [100], while fcc materials tend to fail in shear prior to tensile instability when pulled in that direction. The former result helps to explain {100} cleavage in bcc metals, while the latter is consistent with the ductility of fcc metals (though the axial symmetry of their applied tension precludes the {111} slip that is ordinarily observed in fcc). They found that fcc metals were relatively weak when pulled in [110], a prediction that is not borne out by the limited pseudopotential work that is now available. The crystallography of the failure modes is clearly important, and we shall discuss it in the following section.

Ab initio pseudopotential studies of tensile strain in some of the same materials were done by Sob, et al. [33-34], by Li and Wang [35] and by the present authors [30-31]. For W in fully relaxed tension along [100], Sob, et al. [33] calculate a strength of 28.9 GPa ($0.07E_{100}$). As expected, this value is much lower than the strength in a stretch along [111], the other case they studied. Our own result for W in [100] tension is almost identical, 29 GPa [30].

In other work, Sob et al. [34] studied relaxed tension in Cu and NiAl. They calculated a very high tensile strength for Cu, 33 GPa for stretch along [100], 31 GPa for [110] and 29 GPa for [111]. These results are almost certainly unrealistic; such stresses would produce shear stresses on the slip system ⟨112⟩{111} that are several times the ideal strength in shear [28]. However, the value for the tensile strength along [110] is interesting for the separate reason that it differs so dramatically from the value computed by Milstein and Chantasiriwan [32] (5.47 GPa), and does not show the relative weakness in [110] these investigators found for all fcc's they studied. The discrepancy is puzzling since the low strength along [110] was interpreted [32] as a consequence of fcc symmetry. The subject deserves further study.

Li and Wang [35] studied the relaxed stretch of Al along [100] and [111]. They found high strength in tension, but they also found that shear instability intruded before tensile failure. For example, the first failure in a relaxed stretch along [100] is an orthorhombic shear ($\varepsilon_3 = -\varepsilon_2$) at a tensile strain of 27% and a tensile load of 12.1 GPa (Milstein and Chantasiriwan's [32] value is 11.1 GPa). Note, however, that this tensile stress imposes a shear stress of 5.7 GPa on the $[\bar{2}11](111)$ system, which is several times the ideal strength in shear on this system (1.85 GPa) [28]. This result re-emphasizes the fact that the calculated strength for a stretch on an axis of high symmetry is strongly influenced by the symmetry itself.

Table III: Calculations of the ideal strength (GPa) in tension. E is Young's modulus in the tensile direction. Where a shear instability has been found before tensile failure, its stress, σ*, is also listed.

material	cell	ref	axis	σ(σ*)	σ/E (σ*/E)
W	bcc	33	[100]	28.9	0.071
		30	[100]	29.0	0.071
Fe	bcc	31	[100]	12.5	0.08
		32	[100]	5.5	0.05
Al	fcc	35	[100]	12.5 (12.1)	0.20 (0.19)
		35	[111]	11.0	0.15
		32	[100]	12.6 (11.1)	0.20(0.17)
		32	[111]	14.8	0.20
		32	[110]	4.18	0.06
Cu	fcc	34	[100]	33	0.49
		34	[111]	29	0.15
		34	[110]	31	0.24
		32	[100]	23.7(9.82)	0.35(0.15)
		32	[111]	26.5	0.14
		32	[110]	5.47	0.04

We [31] have recently completed an *ab initio* calculation of the ideal strength of Fe in tension along [100]. This calculation is made difficult by the need to include the non-local effects of the magnetic interaction; calculations that do not include these effects (for example, Craivich, et al. [36]) yield the unphysical result that bcc Fe is mechanically unstable in the low-temperature limit. Our calculations predict an ideal strength of ≈10.5 GPa ($0.08E_{100}$), for Fe in relaxed tension on [100]. The ideal strength of Fe is, in dimensionless form, very close to that of W ($0.07E_{100}$), despite the difference in the nature of bonding. As we shall discuss below, this result reflects the strong influence of crystal symmetry.

Cohesive energy calculations. A number of investigators have calculated the cohesive energies of various elements and compounds as functions of their atomic configurations (refs. [23,36-41], among many others). Most of this work has been done to study structural phase transformations. If the calculated energies are plotted as functions of strain, the conjugate stresses can be extracted from them and used to estimate the ideal strength. However, the published data do not allow the reader to do this with much accuracy.

Understanding the ideal strength

While the *ab initio* calculations are limited in number, they show two clear trends. First, the ideal strength in a particular deformation mode is proportional to the modulus that governs linear elastic deformation in that mode. Second, the constant of proportionality is set by the crystal structure. Both trends reflect the crystallographic constraints on elastic stability.

Crystallographic considerations: "the scent of an extremum"

To understand how crystal structure influences ideal strength it is useful to consider stability with respect to uniaxial stress in a particular direction in the six-dimensional space of the Voigt strains. Let e_α be the strain along the axis of load. If we plot the energy as a function of the strain, as in Fig. 4, then the Lagrangian stress is given by the slope of the curve, $\tau_\alpha(e_\alpha) = \partial E/\partial e_\alpha$, and is approximately equal to the Cauchy stress, t_α, if the strain is not too large. The intrinsic value of the ideal strength on this path is given by the first maximum of the Cauchy stress, which is roughly coincident with the first inflection point on $E(e_\alpha)$. While we shall stay with the one-dimensional case for illustrative purposes, the argument is easily generalized to consider instability with respect to off-axis strain increments. It follows that the study of elastic instability is intimately associated with the study of inflection points in the function $E(\mathbf{e})$.

While "accidental" inflection points are always possible, an inflection point in the strain-energy relation usually falls between extrema whose positions are fixed by symmetry. At least three types of extrema are possible in the one-dimensional case (Fig. 5): (1) the extremum at infinity; in the limit of hydrostatic tension the energy becomes stable because the atoms are arbitrarily far apart; (2) an extremum separating identical structures that are related by shear or rotation; (3) an extremum between different structures that are connected by a structural phase transformation. In each of these cases, the extremum creates an elastic instability that limits the mechanical strength of a solid strained in its direction.

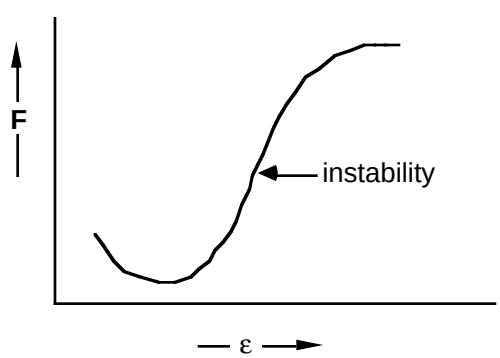

Fig. 4: Cohesive energy as a function of strain showing instability at the point of inflection.

Note that, in general, the extremum that creates an elastic instability has no particular physical significance beyond the fact that it does that. The extremal state will almost never be reached, since the solid becomes unstable before arriving at it. If the extremum were reached it could not be preserved by natural means, since it is unstable. The strength is determined by the proximity of the extremum (the "scent of the extremum") rather than the extremum itself.

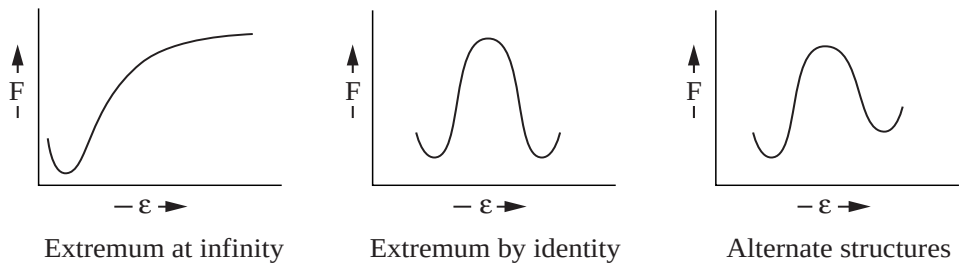

Fig. 5: Three types of extrema determined by the dependence of cohesive energy on strain.

The crystallographic extrema that are associated with particular crystal structures have been studied by a number of investigators, most of whom were interested in structural phase transformations. Milstein and co-workers [10-11, 32, 42-43] offer extensive discussions of the extrema that determine the ideal strength in tension. Sob, et al. [34,44] have added interesting observations on the symmetry of tensile instabilities in simple intermetallics. Shear instabilities have received less attention.

In the following we discuss a few specific instabilities that have important metallurgical implications.

<u>{100} cleavage in bcc</u>

One of the more unfortunate facts in the history of technology is the tendency of Fe to fracture in a brittle mode at low temperature. This behavior, which is responsible for the ductile-brittle transition in iron and steel, is due to the fact that Fe cleaves with relative ease on {100} planes. It shares this behavior with other bcc metals, but not with fcc metals, which suggests that the source is crystallographic. Since {100} is not the close-packed plane in bcc it is superficially puzzling that it should be the preferred cleavage plane.

The reason that bcc metals might prefer to fracture on {100} planes is, however, obvious when one considers the limit of strength [43]. As illustrated in Fig. 6, a relaxed distortion along [001] is precisely the "Bain strain" that connects the bcc and fcc lattices in martensitic transformations [45]. If the bcc structure is stable and the fcc is unstable, as is the usual case for bcc metals, then the bcc crystal becomes elastically unstable when strained about halfway to the fcc structure along [001].

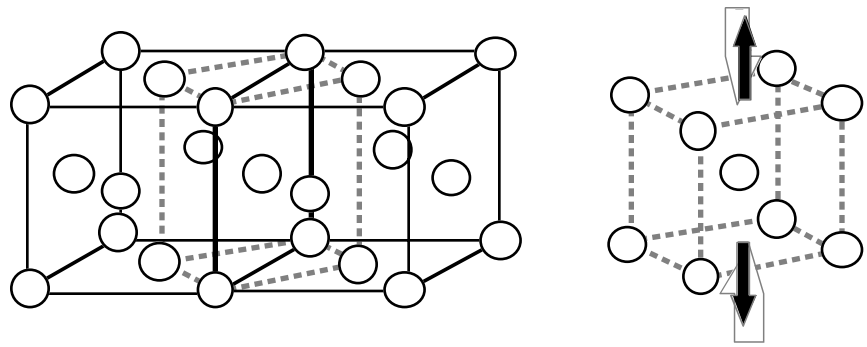

Fig. 6: The fcc structure can be referred to the bct cell outlined in the figure at left. It follows that fcc can be reached by stretching bcc along [001], as shown at right.

It is useful to carry this analysis further. If we assume constant volume, a bcc structure is deformed into fcc by a relaxed engineering strain of 0.26 along [001]. Hence the instability is encountered at a strain of about 0.13. The tensile stress, σ, vanishes in both the bcc and fcc states. If we follow Frenkel [12] and Orowon [6] in assuming a sinusoidal form for the stress-strain curve, the stress (σ) is given by

$$\sigma = \sigma_m \sin\left[\frac{\pi\varepsilon}{0.26}\right] \tag{18}$$

where ε is the strain and σ_m is the maximum stress, the ideal strength in tension along [001]. In the limit of small strain, $\sigma = E\varepsilon$, where E is the modulus for [001] strain. It follows that

$$\sigma_m \approx \frac{0.26E}{\pi} = 0.08E \tag{19}$$

Eq. (19) is very close to the result obtained by Sob, et al. [33] and the present authors [30] for W, and by the present authors for Fe [31].

Note that the Bain strain is asymmetric; the fcc-bcc transformation happens when the fcc crystal is compressed along [001], but not when it is extended. In fact, it does not appear that any crystallographic extremum is reached by small tensile strain in an fcc crystal [32]. It is true that the bcc structure can be made by a fully relaxed strain along [110], which is responsible for the low tensile strengths calculated by Milstein and Chantasiriwan [31] for this mode. But even those stresses are high enough that the shear strength on the most favorable {111} planes would be exceeded before they were reached. While the subject needs further investigation, we note that the fcc-bcc transition via stretch on [110] requires a very large Poisson contraction along [100], which leads us to question the applicability of EAM potentials that were fit at small strains. The sole relevant *ab initio* calculation known to us, that by Sob, et al. [34] for fcc Cu, suggests that this crystal is relatively strong in tension on [110].

"Pencil glide" in bcc

A second puzzling observation about the deformation of bcc crystals is the variety of possible slip planes [46]. While the direction of slip is ordinarily ⟨111⟩, the slip plane can be {110}, {112} or {123}, and sometimes appears to be such a mixture of these planes and others that the slip plane is left undermined and the deformation is described as "pencil glide". While pencil glide is due to the behavior of mobile dislocations, the ideal strength in shear has a very similar behavior, and it has a simple explanation.

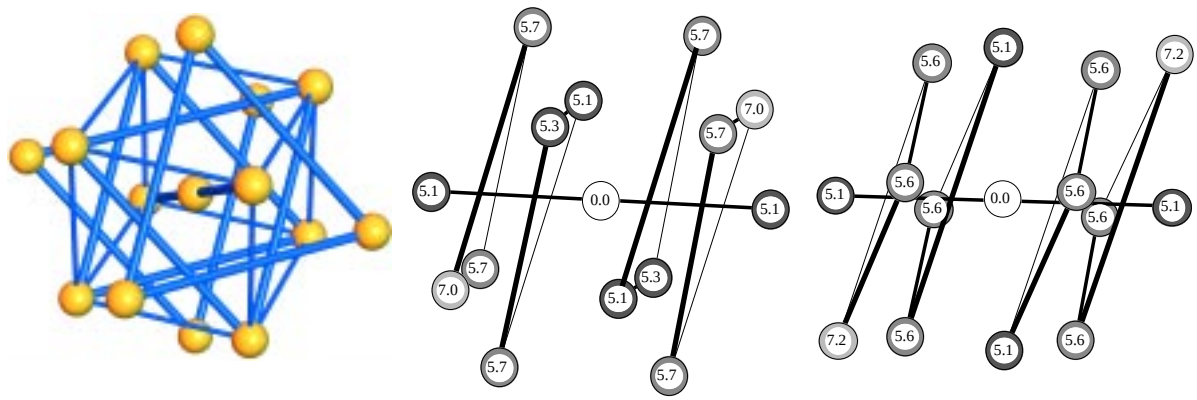

(a) (b) (c)

Fig. 7: a) illustration of the ABCABCA stacking sequence in bcc along the 111 direction. b) illustration of the monoclinic saddle point relaxation for 110 slip (4 neighbors at 5.1 Å, 2 neighbors at 5.3 Å, and 6 neighbors at 5.7 Å). c) illustration of the orthorhombic saddle point relaxation for 112 and 123 slip (4 neighbors at 5.1 Å and 8 neighbors at 5.6 Å).

We have already referenced results showing that in W [29] the ideal shear strengths for the slip systems ⟨111⟩{110}, ⟨111⟩{112} and ⟨111⟩{123} are almost the same. Krenn [31] has recently identified the crystallographic reason for this behavior, which is illustrated in Fig. 7. If we look along the [111] slip direction, the bcc atoms form equilateral triangles centered on [111] (Fig. 7a). Homogeneous shear on a plane that contains the [111] axis has the effect of tilting the coordination triangles in the [111] direction about an axis that lies in the plane of shear, as illustrated in the figure. In a relaxed shear in ⟨111⟩[10$\bar{1}$], the nearest-neighbor coordination of the central atom is disrupted (the symmetry is triclinic), but is partially restored after a strain of 0.34, at which point the crystal has six nearest neighbors per atom and monoclinic symmetry (Fig. 7b). If the shear is in the system ⟨111⟩(11$\bar{2}$) or ⟨111⟩(12$\bar{3}$) a slightly different intermediate extremum is reached, again at a shear of 0.34. This configuration has eight nearest neighbors and orthorhombic symmetry (Fig. 7c). In all three cases, the instability is located about halfway between the origin and the symmetry point at a shear of ≈0.17 [30].

As in the previous example, we can estimate the ideal shear stress by assuming a sinusoidal stress-strain relation with a stress that vanishes at both extrema. The result is

$$\tau = \tau_m \sin\left[\frac{\pi\gamma}{0.34}\right] \tag{20}$$

Since $\tau = G\gamma$ at small strains, where G is the appropriate shear modulus, the ideal shear strength is

$$\tau_m \approx \frac{0.34G}{\pi} = 0.11G \tag{21}$$

which is very close to the value computed *ab initio* for both W and Mo [30,31]. Since W is almost isotropic, the ideal strengths on the three glide systems are almost the same [30]. In less isotropic bcc crystals the ideal strength should vary with the value of the modulus, G. We do not yet have data to test this hypothesis.

Shear in fcc

In fcc the energy extremum that is closest to the origin in the (111) slip plane lies in the $\langle 11\bar{2}\rangle$ direction. If we ignore relaxation this extremum is reached at an engineering strain of 0.33, suggesting an instability at $\gamma = 0.16$. A sinusoidal stress based on this strain (eq. 20) would yield an ideal strength of 0.11G, which is too high (though very close to the original Frenkel value). However, as noted in Table II, there is a significant relaxation of the strain in both Al and Cu, with the consequence that the instability strain drops to .145 for Al and 0.13 for Cu. If we approximate the stress by a sinusoid like eq. 20, adjusted so that the maximum stress falls at the instability strain, we obtain

$$\tau_0(\mathrm{Al}) \approx \frac{0.29G_r}{\pi} = 0.09G_r \tag{22}$$

$$\tau_0(\mathrm{Cu}) \approx \frac{0.26G_r}{\pi} = 0.08G_r \tag{23}$$

which reproduce the results of the *ab initio* calculation.

It follows from the above that one can estimate the ideal strength if one knows the strain that induces elastic instability. In all of the cases examined to date, the ideal strength is well approximated by the maximum stress in a sinusoidal stress-strain relation that fits Hooke's Law at small strains and has its maximum at the instability strain.

Achieving the ideal strength

The final question is whether the ideal strength is a theoretical abstraction or a meaningful parameter that is actually approached in engineering materials. As we shall discuss below, there are at least some cases in which the strength clearly does approach the ideal value, and others in which it may. We specifically consider the strength in shear. If the ideal shear strength is to be achieved, it must be possible to strain the material to elastic instability

before the stress can be relieved by normal dislocation flow. This can happen for any of four reasons: (1) The material is inherently so hard that dislocations cannot move at stresses below the ideal strength. (2) The material is microstructurally strengthened to the point that dislocations cannot move at stresses below the ideal strength. (3) The material contains no dislocations. (4) The strain is imposed so quickly that dislocations cannot respond. The first three possibilities are discussed below. We have not yet investigated the case of high-rate loading, which is complicated by the concurrent increase in temperature.

Inherently "hard" materials

A minimum value of the shear stress is required to move a dislocation through a crystal. While this stress is not well known, it is roughly measured by the Peierls-Nabarro stress, the stress required to move a length of dislocation from one crystallographically stable configuration to another. The simple form of the Peierls-Nabarro stress is

$$\frac{\tau_P}{G} = \frac{2}{1-\nu} \exp\left[-\frac{2\pi}{1-\nu}\left(\frac{h}{b}\right)\right] \tag{24}$$

where h is the spacing between slip planes and b is the Burgers' vector. It is generally agreed that this relation is incomplete, and the correct expression is a subject of active study [47-51]. Still, the simple form does provide a reasonable fit to the available experimental data, as illustrated in Fig. 8 [49]. Its dominant feature is the exponential dependence on (h/b), which is at least qualitatively retained in the more sophisticated models.

As Fig. 8 shows, the crystallographic factor, h/b, depends on the structure, and decreases significantly on moving from the fcc and bcc structures of the common metals to the NaCl and diamond cubic structures of the familiar "hard" materials. Both eq. (24) and more recent theoretical [51] and experimental [52] work suggest that the Peierls stress exceeds 0.1G in the diamond cubic structure, and may reach several percent of G in materials with the NaCl structure. These numbers are in the range of the ideal strength in shear.

Recent research on Si, in particular, strongly suggests that its low-temperature deformation is governed by its ideal strength. Dislocation motion is not observed at low temperature [53]. Moreover, when the material is forced to deform plastically in indentation tests it deforms by structural phase transformation rather than dislocation flow [54,55]. While "hard" materials with the NaCl structure have been less extensively studied, at least some of them have been reported to behave in a similar way. For example, Williams' classic study of the deformation of TiC [56] found no evidence for dislocation glide at low temperature, even when plasticity was forced by microindentation. However, indentation pits released a shower of dislocations on subsequent heating, showing that extensive local lattice deformation had occurred. It hence appears that at least the diamond cubic materials and some of the hard carbonitrides are "inherently hard".

There is a second, well-known class of "inherently hard" materials that deform at (or close to) the ideal strength, even though they are not particularly strong. This class includes materials that deform by stress-induced martensitic transformations [57]. When a material

is in a structure that is only marginally stable an appropriate stress can easily force the barrier, creating “transformation-induced plasticity” at stresses well below those required to move dislocations. The phenomenon of "superelasticity" in materials like nitanol is based on this behavior [58].

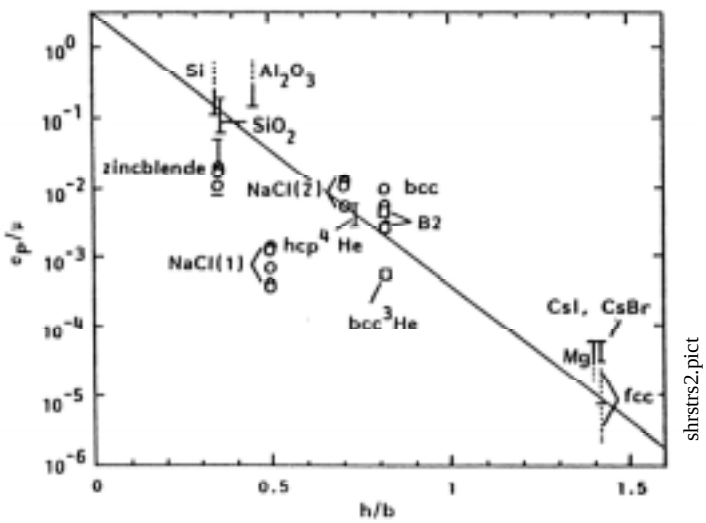

Fig. 8. Normalized Peierls stresses (σ_P/μ) at zero temperature as a function of the crystallographic factor h/b. From Ref. 47.

<u>Microstructurally hardened materials</u>

If a material does not have the inherent strength to reach the elastic limit then one may use various microstructural mechanisms to harden it further. The most obvious mechanisms are grain refinement, which strengthens through the Hall-Petch effect, work hardening, which strengthens by adding "forest" dislocations, and precipitation hardening.

Research on the Hall-Petch effect suggests that grain refinement cannot harden to ideal strength, at least in conventional structural metals. Not only is it difficult to achieve grain sizes that are small enough to produce ideal strength, but the strength is also limited by grain-boundary dominated processes when the grain size becomes very small; the strength asymptotes, and may even decrease for smaller sizes [59]. For example, Kimura, Takaki and co-workers [60-62] find the Hall-Petch relation for Fe to be given roughly by

$$\sigma_y = 0.15 + 0.54d^{-1/2} \tag{25}$$

where σ is in GPa and d is the grain size in microns. If we take the ideal shear strength of Fe to be 0.11G, as it is for W and Mo, then $\tau_c \approx 6.6$ GPa, and σ_y would have to exceed 13 GPa before the ideal shear strength would be reached on even the most favorable possible slip plane. To achieve this value, the grain size would have to fall below 2 nm. The smallest grain size reported by Kimura, et al. [60] is about 20 nm, with $\sigma_y < 4$ GPa. Jang

and Koch [63] previously reported achieving grain sizes near 6 nm with $\sigma_y \approx 9$ GPa, but these still remain well below ideal. While the actual mechanisms that limit strength at ultra-fine grain size remain controversial [64,65], it does not appear that the ideal strength can be reached in this way.

Work-hardening and precipitation-hardening strengthen the crystal by introducing defects that act as obstacles to dislocation motion: "forest" dislocation in the case of work hardening, small inclusions in the case of precipitation hardening. In the conventional case these behave as isolated barriers [66]. If their mean separation is l_s, the increment to the shear strength is

$$\frac{\Delta\tau_c}{G} = \alpha\frac{b}{l_s} \tag{26}$$

where α measures the effective resistance offered by the obstacle (the "obstacle strength"). For dislocations, a reasonable value for α is in the range 0.1-0.3, while for impenetrable precipitates that have almost equal size (the strongest morphology [67]), α has a maximum value of about 0.7 [68]. To achieve $\Delta\tau_c \approx 0.1G$ by dislocation hardening would, therefore, require a dislocation spacing less than 3b; to do it with precipitation hardening would require a precipitate spacing less than about 7b. Neither seems achievable.

On the other hand, it may be possible to approach the ideal strength by hardening with precipitates at high volume fraction, where deformation requires dislocation flow through the narrow interstices of the particles. This seems to be the approach recently used by Knapp, et al. [69] to achieve very high indentation strength in oxide-strengthened aluminum. It is not yet clear how close they have come to the theoretical limit.

Defect-free materials

There are two ways to make defect-free samples for experimentation: to grow small, defect-free crystals ("whiskers"), or to do indentation tests with "nanoindenters" that are so small in diameter that they probe volumes that lie between mobile defects.

Since the classic work of Brenner [15], whisker measurements have been widely cited as the standard of maximum strength. However, as it has become possible to calculate the ideal strength it has become increasingly clear that whisker strengths do not approach the ideal value all that closely. For example, Brenner's highest values for the critical resolved shear stress of Cu is 0.85 GPa, his value for Fe is 3.56 GPa., and the highest value obtained on W whiskers [70] is about 11 GPa. All these values are substantially below the ideal strength (Table I). A close reading of Brenner's work makes it understandable that this should be the case. Whiskers are small crystals with very high surface-to-volume ratios, and Brenner noted that their deformation appeared to initiate at the surface in every case. The deformation process that competes with elastic instability in a defect-free crystal is the spontaneous nucleation of dislocations [71]. Since dislocations are most easily

formed by heterogeneous nucleation at free surfaces, this mechanism, rather than elastic instability, is likely to limit the strength of defect-free crystals.

The alternate method for testing defect-free material is nanoindentation [72-75], which is, essentially, a microhardness test done with a nano-tipped indenter. The tip is instrumented to record load-displacement data. Until the substrate yields, the deformation field of the indenter should be approximately Hertzian [76], which makes it possible to use the data to infer the stresses and strains at which yielding occurred. Moreover, since the maximum shear in a Hertzian strain field is well beneath the surface, nanoindentation tests can avoid early yielding by dislocation emission from the surface (barring surface damage from the indenter [77]).

Nanoindentation tests have produced hardnesses that suggest yield at very near the ideal strength in a variety of metals, including Au [78], W [76], Mo [79] and oxide-strengthened Al [69]. Some of the reported values, in fact, exceed the ideal strength. For example, Bahr, et al. [76] report data showing shear stresses as high as 28 GPa in W prior to yielding, well beyond the value (18 GPa) that corresponds to the ideal strength on any of the common slip planes. The interpretation of this data is complicated by the absence of a detailed stress analysis of the indentation field. Not only are triaxial stresses present, which may change the ideal strength, but the moduli soften dramatically as the ideal strength is approached, introducing unknown errors in the Hertzian stress.

A recent analysis by Roundy [30] suggests that most of the discrepancy between the computed ideal shear strength and the values inferred from Hertzian analyses of the best nanoindentation data may be attributable to the softening of the moduli. He assumes that the Hertzian solution gives a reasonable approximation to the strain field, but, because of the softened moduli, mis-estimates the stress at the instability. Using sinusoidal stress-strain dependence, he obtains

$$\tau_m = \left[\frac{2}{\pi}\right] \tau_H \tag{27}$$

where τ_m is the ideal shear strength and τ_H is the instability stress inferred from the Hertzian stress field. With this correction, the maximum Hertzian stress measured by Bahr, et al. [76] for W, 28 GPa, corresponds to a shear strength of 17.8 GPa, very close to the theoretical result.

Conclusion

Given powerful new tools for both experimental and theoretical analysis, and important new incentives to study the behavior of nearly perfect materials, the ideal mechanical strengths of materials will become an increasingly active subject of research in the coming years. The problem is as interesting as it is important.

Acknowledgment

The authors appreciate very helpful discussions with Daryl Chrzan, Dept. of Materials Science, Steven Louie and Seung-Hoon Jhi, Dept. of Physics, Univ. of California, Berkeley, and with Sidney Yip, Dept. of Nuclear Engineering, MIT. This work was supported by the Director, Office of Energy Research, Office of Basic Energy Sciences, U.S. Department of Energy, under Contract No. DE-AC03-76SF00098.

References

1. J.W. Gibbs, Trans. Conn. Acad., 3, 108-248 (1876) (Scientific Papers of J. Willard Gibbs, Vol. 1: Thermodynamics, Ox Bow Press, 1993, p. 184-215)
2. A. Kelly and N.H. Macmillan, Strong Solids, 3rd ed., Clarendon Press, Oxford (1986)
3. M. Polanyi, Z. Physik, 7, 323 (1921)
4. F. Zwicky, Phys. Zeit., 24, 131 (1923)
5. M. Born and R. Furth, Proc. Camb. Philos. Soc., 36, 455-65 (1940)
6. E. Orowon, Rept. Prog. Phys., 12, 185 (1949)
7. N.H. Macmillan and A. Kelly, Proc. Roy. Soc. (London), A330, 291-308 (1972)
8. N.H. Macmillan and A. Kelly, Proc. Roy. Soc. (London), A330, 309-317 (1972)
9. F. Milstein, J. Appl. Phys., 44, 3833-40 (1973)
10. F. Milstein and K. Huang, Phys. Rev. B, 18, 2529-41 (1978)
11. F. Milstein, R. Hill and K. Huang, Phys. Rev. B., 21, 4282-91 (1980)
12. J. Frenkel, Z. Phys., 37, 572 (1926)
13. J.K. Mackenzie, PhD. Thesis, Bristol University (1949)
14. K. Huang, F. Milstein and J.A. Baldwin, Jr., Phys. Rev. B, 10, 3635-46 (1974)
15. S.S. Brenner, J. Appl.Phys., 27, 1484 (1956)
16. R. Hill, Math. Proc. Camb. Phil. Soc., 77, 225-240 (1975)
17. R. Hill and F. Milstein, Phys. Rev. B, 15, 3087-97 (1977)
18. J. Wang, S. Yip, S.R. Phillpot and D. Wolf, Phys. Rev. Lett., 71, 4182-85 (1993)
19. J. Wang, J. Li, S. Yip, S. Phillpot and D. Wolf, Phys. Rev. B, 52, 12,627-35 (1995)
20. J. Wang, J. Li, S. Yip, D. Wolf and S. Phillpot, Physica A, 240, 396-403 (1997)
21. J.W. Morris, Jr. and C.R. Krenn, Phil. Mag. A (in press)
22. D.C. Wallace, Thermodynamics of Crystals, J. Wiley, New York, 1972, p. 14-32.
23. B. N. Harmon, in Statics and Dynamics of Alloy Phase Transformations, eds. P.E.A. Turchi and A. Gonis, Plenum, New York, 1994, p. 421-34
24. M.L. Cohen, Phys. Scr., T1, 5 (1982)
25. A.T. Paxton, P. Gumbsch and M. Methfessel, Phil. Mag. Lett., 63, 267-274 (1991)
26. W. Xu and J. A. Moriarty, Phys. Rev. B., 54, 6941-51 (1996)
27. P. Söderlind and J.A. Moriarty, Phys. Rev. B, 57, 10340-350 (1998)
28. D. Roundy, C.R. Krenn, M.L. Cohen and J.W. Morris, Jr., Phys. Rev. Lett., 82, 2713-16 (1999)

29. C.R. Krenn, D. Roundy, J.W. Morris, Jr. and M.L. Cohen, LBNL Rept. #42950 (1999) (Mat. Sci. Eng. A (in press))
30. D. Roundy, C.R. Krenn, M.L. Cohen and J.W. Morris, Jr., LBNL Rept. #44373, (1999) (submitted)
31. D. Roundy, C.R. Krenn, M.L. Cohen and J.W. Morris Jr., unpublished research
32. F. Milstein and S. Chantasiriwan, Phys. Rev. B, 58, 6006-18 (1998)
33. M. Sob, L.G. Wang and V. Vitek, Mat. Sci. Eng., A234-236, 1075-78 (1997)
34. M. Sob, L.G. Wang and V. Vitek, Kovove Materialy, 36, 145-52 (1998)
35. W. Li and T. Wang, J. Phys.: Condensed Matter, 10, 9889-9904 (1998)
36. P.J. Craievich, M. Weinert, J.M. Sanchez and R.E. Watson, Phys. Rev. Lett., 72, 3076-79 [1994]
37. M.J. Mehl and L.L. Boyer, Phys. Rev. B, 43, 9498 (1991)
38. P. Söderlind, O. Eriksson, B. Johansson, J.M. Wills and A.M. Boring, Nature, 374, 524-25 (1995)
39. S. Jeong, Phys. Rev. B, 53, 13973 (1996)
40. P. Alippi, P.M. Marcus and M. Scheffler, Phys. Rev. Lett., 78, 3892-95 (1997)
41. P. Söderlind, J.A. Moriarty and J.M. Wills, Phys. Rev. B, 53, 14063-72 (1996)
42. F. Milstein and D. Rasky, Phil. Mag. A, 45, 49-61 (1982)
43. F. Milstein and J. Marschall, Phil. Mag. A, 58, 365-84 (1988)
44. M. Sob, L.G. Wang and V. Vitak, Comp. Mat. Sci., 8, 100-106 (1997)
45. A.G. Khatchaturyan, Theory of Structural Transformations in Solids, J. Wiley, New York, 1983
46. J.W. Christian, Met. Trans. A, 14A, 1237-56 (1983)
47. F.R.N. Nabarro, Proc. Phys. Soc. (London), 59, 256 (1947)
48. H.B. Huntington, Proc. Phys. Soc., B68, 1043 (1955)
49. K. Ohsawa, H. Koizumi, H.O.K. Kirchner and T. Suzuki, Phil. Mag., 69, 171-181 (1994)
50. F.R.N Nabarro, Phil. Mag., 75, 703-711 (1997)
51. B. Joos and M.S. Duesbery, Phys. Rev. Lett., 78, 266-69 [1997]
52. M.S. Duesbery and B. Joos, Phil. Mag. Lett., 74, 253 (1996)
53. R.H. Folk II, M. Khantha, D.P. Pope and V. Vitek, in Fracture and Ductile-Brittle Behavior, G.E. Beltz, R.L. Blumberg-Selinger, K.-S. Kim and M.P. Marder, eds., MRS, Pittsburgh, 1999, p. 161-68
54. D.R. Clarke, M.C. Kroll, P.D. Kirchner, R.F. Cook and B.J. Hockey, Phys. Rev. Lett., 60, 2156 (1988)
55. K. Minowa and K. Sumino, Phys. Rev. Lett., 69, 320 (1992)
56. W. S. Williams, Solid State Chem., 6, 57-118 (1971)
57. C.M. Wayman and H.K.D.H. Bhadesia, in Physical Metallurgy, R.W. Cahn and P. Haasen, eds., North-Holland, Amsterdam (1996), vol. 2, p. 1531-44
58. C.M. Wayman, in Advanced Materials, K. Otsuka and K.I. Shimizu, eds., MRS, Pittsburgh, 1989, p. 63-76
59. S. Yip, Nature, 391, 532-33 (1998)
60. Y. Kimura and S. Takaki, Mat. Trans. JIM, 36, 289-96 (1995)
61. Y. Kimura and S. Takaki, in Proc., 1998 PM World Congress: Nanocrystalline Materials, 1998, p. 573-78

62. Y. Kimura, S. Takaki, S. Suejima, R. Uemori and H. Tamehiro, ISIJ Int., 39, 176-182 (1999)
63. J.S.C. Jang and C.C. Koch, Scr. Metall. Mater., 24, 1599-1604 (1990)
64. P.G. Sanders, J.A. Eastman, and J.R. Weertman, Acta Mater., 45, 4019-25 (1997)
65. M. Furukawa, Y. Iwahashi, Z. Horita, M. Nemoto, M, N.K. Tsenev, R.Z. Valiev and T.G. Langdon, Acta Mater., 45, 4751-57 (1997)
66. U.F. Kocks, A.S. Argon and M.F. Ashby, Thermodynamics and Kinetics of Slip, Vol. 19 of Progress in Materials Science, Pergamon, Oxford (1975)
67. J. Glazer and J.W. Morris, Jr., Phil. Mag. A, 56, 507 (1987)
68. D.J. Bacon, U.F. Kocks and R.O. Scattergood, Phil. Mag. A, 28, 1241 (1973)
69. J.A. Knapp, D.M. Follstaedt and S.M. Myers, J. Appl. Phys., 79, 1116-22 (1996)
70. I.M. Mikhailovskii, P.Y. Poltinen and L.I. Federova, Sov. Phys. Solid State, 23, 757 (1981)
71. J.P. Hirth and J. Lothe, Theory of Dislocations, 2nd Ed., J. Wiley, New York (1982)
72. N. Gane and F.P. Bowden, J. Appl. Phys., 39, 1432 (1968)
73. J.B. Pethica and W.C. Oliver, Phys. Scripta, T19, 61 (1987)
74. M.F. Doerner and W.D. Nix, J. Mat. Res., 1, 601-609 (1986)
75. W.C Oliver and G.M. Pharr, J. Mater. Res., 7, 1564-83 (1992)
76. D.F. Bahr, D.E. Kramer and W.W. Gerberich, Acta Mater., 46, 3605-17 (1998)
77. A.B. Mann and J.B. Pethica, Phil. Mag. A, 79, 577-92 (1999)
78. J.D. Kiely and J.D. Houston, Phys. Rev. B, 57, 12588-594 (1998)
79. W.D. Nix, Dept. Materials Science, Stanford Univ., Private Communication, 1999